

Proxy-Based Haptic Rendering for Underactuated Haptic Devices

Daniel Lobo¹, Mine Sarac², Mickeal Verschoor¹, Massimiliano Solazzi², Antonio Frisoli², Miguel A. Otaduy¹

Abstract—Standard haptic rendering algorithms are not well suited for underactuated haptic devices. They compute forces oblivious of underactuation, and then they simply project the resulting forces to the actuated subspace. We propose instead a proxy-based haptic rendering method that computes displacements in the actuated subspace only, and then translates these displacements into force commands using regular controllers. Our method is well behaved in two important ways: it is locally passive w.r.t. the motion of the haptic device, and the displayed impedance can be easily controlled regardless of the mapping between device and virtual configuration spaces.

I. INTRODUCTION

Most haptic rendering algorithms follow a common, well-established methodology, that renders contact between a virtual object and a virtual environment by simulating the object as a proxy of the haptic device. The core idea is simple. The tracked configuration of the haptic device is mapped to a virtual object (a.k.a. haptic probe) in the virtual environment, a proxy of this probe is computed by minimizing the distance to the haptic probe subject to environment constraints, a command force is computed based on the deviation between haptic probe and proxy, the force is mapped back to the device, and finally the force is displayed to the user. This approach assumes an impedance-type device, but can be adopted on admittance-type devices with small modifications.

Such a simple and elegant approach was initially named god-object [33] or virtual proxy [25] in 3-DoF haptic rendering. It was extended for rendering of rigid tools in 6-DoF haptic rendering [17], [19], [31], also for rendering of contact between deformable objects [8], [3], and even for rendering of direct touch by interpreting virtual fingers and hands as haptic probes [10], [23]. A formalization and generalization of the approach can be found in [20].

Proxy-based haptic rendering has reached this level of standardization thanks to the simplicity of stability conditions. If the simulation of the proxy is passive, stability can be enforced simply by appropriate tuning of a controller that links the proxy and the haptic probe [6], [1].

But the standard proxy-based rendering method makes an important assumption. The actuated DoFs of the device match exactly a subset of the DoFs of the proxy. Unfortunately, this assumption does not hold for many interesting haptic systems. On one hand, computational models and resources grow steadily, and we can currently afford interactive simulation of rich and complex haptic proxies,

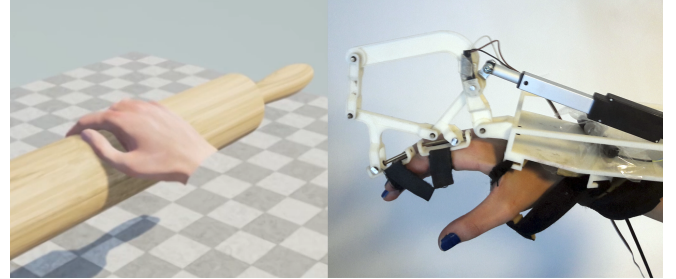


Fig. 1. Contact with a soft hand being rendered through an underactuated exoskeleton.

with many more degrees of freedom than the haptic device [22], [30], [32]. On the other hand, novel designs of exoskeletons exploit complex underactuated mechanisms to maximize wearability, minimize actuators, etc. [13]. In such haptic systems, actuated DoFs may not map to a subset of the DoFs of the haptic proxy. As we show in the paper, naïve application of proxy-based rendering to underactuated devices produces undesired results.

We present an extension of the proxy-based haptic rendering algorithm for general underactuated devices. The core conceptual novelty is to define two instances of the proxy: one, as usual, fully simulated and constrained by the virtual environment; the other one constrained to the subspace defined by the DoFs of the device, where actuated and non-actuated DoFs are trivially separable. Thanks to the subspace proxy, we can compute feedback haptic commands that are optimally constrained to actuated DoFs, and we can do this using regular controllers as in the standard rendering method. Moreover, our formulation is general. It admits haptic and virtual configuration spaces of different dimensionality, and connected through nonlinear mappings.

We express our rendering algorithm using a general optimization formulation. This approach enables simple and elegant formulation and interpretation, and it leaves the mathematical and implementation details to each particular type of device, virtual proxy, and objective function. Nonetheless, we describe a particular implementation using an underactuated finger exoskeleton [27], [26] for haptic rendering of soft grasping interactions, as shown in Fig. 1.

After a discussion of related work, we focus on the analysis of standard proxy-based haptic rendering from the standpoint of haptic and virtual configuration spaces. Then, we extend the analysis to underactuated haptic devices, and we formulate our novel subspace-proxy-based haptic rendering method. The full formulation requires the solution

¹Dept. of Computer Science, Universidad Rey Juan Carlos, Madrid, Spain

²PERCRO, Scuola Superiore Sant'Anna, Pisa, Italy

to a nonlinear optimization problem, and we introduce an extension that uses linearized device kinematics to yield a quadratic optimization problem with a computationally efficient closed-form solution.

We carry out a theoretical analysis that validates the benefit of our method over other approaches. We evaluate the displayed impedance of our method in contrast to standard proxy-based haptic rendering and to a projection to the null-space of non-actuated DoFs. Our method offers unconditional passivity, and it also enjoys configuration-independent displayed impedance, which helps maximize transparency. To conclude, we show the application of our general formulation to the underactuated finger exoskeleton.

II. RELATED WORK

a) Underactuated Exoskeletons: Underactuation is a common strategy for building cost-effective robotic devices, in particular exoskeletons and grippers. However, such robotic devices have been used typically for rehabilitation or for force augmentation, not for haptic rendering. Therefore, their control strategies are designed to favor the motion of the user, not to oppose it. Laliberté et al. [13] presented one of the first underactuated robotic hands. Their control problem required the definition of the pose for a target hand configuration based on the object to be grasped, and then they applied a PD controller to guide the hand to this pose. Birglen et al. [4] issued a PD position control loop for the actuator, together with a saturating open-loop force control when grasping was achieved. Fassih et al. [9] proposed a PD control in the joint space, with gravity compensation and the joint elastic torque component. They defined virtual dampers around the passive joints, and they controlled the desired positions with a spring damper. Luo et al. [16] proposed a sliding-mode impedance control for robotic grippers, which required knowledge of the dynamics of the mechanism, and can hardly be extended to exoskeletons due to uncertainty about the human’s model.

The hand exoskeleton that we use [27], [26] performs a PI control on the displacement of a linear actuator, a strategy that has also been adopted by others [11], including for pneumatic actuators [24]. Differ et al. [7] focused on the design of a hand prosthesis instead of grippers. Therefore, their robotic device had to reach a more human-like behavior, and enforcement of stability was a must. They implemented a passivity-based control algorithm, with the dynamics of the controller changing with respect to the contact forces acting on the system in order to balance the total energy.

b) Interaction Using Underactuated Devices: While underactuated exoskeletons are typically not used for haptic rendering, many common haptic devices are indeed underactuated. This is the case, for example, with devices with 6-DoF input (translation and rotation sensing) and 3-DoF output (force—but no torque—actuation). There has been important effort on the analysis of such underactuated haptic devices, also from the point of view of haptic rendering of virtual environments.

Barbagli and Salisbury [2] analyzed underactuated haptic devices in terms of controllability and observability of a virtual environment, and consequently provided guidelines and considerations for the design of a device. However, they did not make an effort at trying to optimize haptic rendering settings for a given haptic device. Verner and Okamura [28] analyzed passivity in asymmetric devices (i.e., those with a different number of controlled and observed DoFs).

The works of Luecke [15] and Meli and Prattichizzo [18] are probably the closest to ours. Luecke considered a haptic device whose end-effector maps exactly to a virtual object, but it is underactuated. Haptic rendering is computed by first defining forces for the virtual object, and then finding optimal control parameters that maximize the similarity between those forces and the ones actually displayed by the device. The solution does not consider cases where the virtual object has a higher dimensionality than the end-effector or cases where the haptic device includes non-actuated DoFs. Meli and Prattichizzo studied methods to render contact forces through an underactuated device, while maximizing task performance. For each task, they defined an optimality criterion in the selection of underactuated feedback. In contrast to theirs, our work stands on proxy-based rendering, but it can accommodate task-dependent metrics in the computation of the proxy.

There are several works that have looked at the use of devices with 3-DoF actuation and 6-DoF sensing for haptic object-object interaction. Verner and Okamura [29] ran experimental analysis of the performance gain provided by torque feedback over force-only feedback. Lee [14] designed a modified penalty-based method that ensures admissible rendered stiffness while correctly balancing directional forces. And Kadlecák et al. [12] used sensory substitution and pseudo-haptic feedback to simulate torque feedback.

III. NOTATION

We denote as $\mathcal{Q} = \mathcal{Q}_a \times \mathcal{Q}_n$ the configuration space of the haptic device, with \mathcal{Q}_a the actuated configuration space (resulting from actuated DoFs), and \mathcal{Q}_n the non-actuated configuration space (resulting from non-actuated DoFs). $\mathbf{q} = (\mathbf{q}_a, \mathbf{q}_n)^T \in \mathcal{Q}$ represents a device state, with $\mathbf{q}_a \in \mathcal{Q}_a$ the state of actuated DoFs, and $\mathbf{q}_n \in \mathcal{Q}_n$ the state of non-actuated DoFs. For ease of notation, we define a selection matrix \mathbf{S} that selects the actuated state from the complete state, i.e., $\mathbf{q}_a = \mathbf{S} \mathbf{q}$.

Similarly, we denote as \mathcal{X} the (unconstrained) configuration space of the virtual object. $\mathbf{x} \in \mathcal{X}$ represents a virtual state.

There is a kinematic mapping $f : \mathcal{Q} \rightarrow \mathcal{X}$ from the configuration space of the device to the configuration space of the virtual object. Then, we can compute a virtual state corresponding to a device state, i.e., $\mathbf{x} = f(\mathbf{q})$. Fig. 2 shows a conceptual representation of the haptic and virtual configuration spaces, together with their mapping. We denote as $\mathbf{J} = \frac{\partial \mathbf{x}}{\partial \mathbf{q}}$ the Jacobian of the mapping f , which allows a linearization of the typically nonlinear mapping f . We also split the Jacobian into $\mathbf{J} = (\mathbf{J}_a, \mathbf{J}_n)$, with $\mathbf{J}_a = \frac{\partial \mathbf{x}}{\partial \mathbf{q}_a}$ and

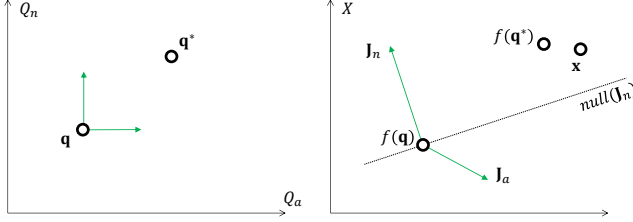


Fig. 2. Schematic representation of the device configuration space \mathcal{Q} (left) and the virtual configuration space \mathcal{X} (right). q represents the device state and $f(q)$ its corresponding configuration in the virtual environment, i.e., the haptic probe; x represents the standard proxy; q^* represents the subspace proxy and $f(q^*)$ its corresponding configuration in the virtual environment. The images also represent the linear subspaces of actuated and non-actuated motion in the virtual environment, J_a and J_n .

$J_n = \frac{\partial x}{\partial q_n}$ the Jacobians w.r.t. actuated and non-actuated DoFs respectively. Only when the number of DoFs of \mathcal{X} and \mathcal{Q} match, J is square, and the mapping f may be invertible.

Finally, we denote as τ a device force vector, and as f a generalized virtual force. For the exposition, we will assume impedance-mode rendering. However, all methods could be applied in admittance-mode rendering by exchanging force commands with position commands.

IV. REVIEW OF PROXY-BASED HAPTIC RENDERING

We start this section with a formal description of the standard proxy-based haptic rendering method. We discuss its major assumptions and the problems induced when the method is applied to underactuated devices, in particular the effects on passivity and rendered impedance. Next, we consider a variation of proxy-based rendering, which computes optimal actuator forces subject to underactuation constraints. We show that, while this method typically satisfies passivity, it yields a configuration-dependent rendering impedance.

A. Standard Rendering Algorithm

Let us define the state of the device q , and the corresponding position of the haptic probe in the virtual environment $f(q)$. Proxy-based rendering computes a proxy x that minimizes the distance to the probe according to a certain metric, subject to environment constraints. Then, the method computes a force $f = Z_x \Delta x$ in the virtual environment, based on a mechanical impedance Z_x and the displacement from the probe to the proxy $\Delta x = x - f(q)$. Next, the force is transformed to the configuration space of the device using the Jacobian transpose approach: $\tau = J^T f$. Finally, forces are displayed.

The standard proxy-based rendering algorithm makes important assumptions about the configuration spaces \mathcal{Q} and \mathcal{X} : their dimensionality is the same, the Jacobian J is hence square, and the mapping f is invertible. This is the case, for example, in typical 3-DoF and 6-DoF haptic rendering systems. In haptic rendering of deformable objects using stylus devices, it is easy to extract a rigid subspace of the full deformable configuration space (using, e.g., rigid modes or a rigid handle), and define this rigid subspace as \mathcal{X} for the purpose of applying the proxy-based rendering algorithm.

B. Analysis for Underactuated Systems

With underactuated devices, even if a full force vector τ is computed, force can obviously be rendered only on actuated DoFs. The effective force resulting from the application of the proxy-based rendering algorithm to an underactuated device is then:

$$\tau_a = J_a^T f = J_a^T Z_x \Delta x. \quad (1)$$

Simple projection of the forces to the actuated DoFs fails to reproduce target forces that lie in the null-space of the actuated DoFs. In some popular types of underactuated haptic systems, it is easy to map the actuated DoFs to a well-defined subspace of the full virtual configuration space, e.g., in systems with 6-DoF input (translation and rotation) and 3-DoF output (force only). In these cases, the Jacobian J is block diagonal, and the forces of virtual DoFs that map to actuated DoFs are matched exactly, while the forces of other virtual DoFs are simply zero.

We can formally analyze the rendering algorithm in terms of the displayed impedance $\frac{\partial \tau}{\partial q}$. The rendering method is passive if the displayed impedance is negative definite, i.e., all its eigenvalues are negative. In the following analysis, we make two approximations. We ignore the local change of the proxy position due to the motion of the device, i.e., $\frac{\partial x}{\partial q} = 0$. And we also ignore the local change of the Jacobian, i.e., $\frac{\partial J}{\partial q} = 0$.

From (1), and with $\tau = S^T \tau_a$, we have:

$$\frac{\partial \tau}{\partial q} = -S^T J_a^T Z_x J. \quad (2)$$

There is no guarantee that the displayed impedance is negative definite.

C. Null-Space Force Optimization

Let us now consider a variation of proxy-based haptic rendering that accounts for underactuation prior to transforming the target force $f = Z_x \Delta x$ to the configuration space of the device. In essence, the method transforms a different force f^* , as close as possible to the target force, but which yields no forces on non-actuated DoFs. The approach can be formulated as a constrained optimization problem:

$$\tau_a = J_a^T f^*, \quad \text{with} \quad (3)$$

$$f^* = \arg \min \|f^* - f\|^2, \quad \text{s.t. } J_n^T f^* = 0,$$

with closed-form solution:

$$\tau_a = J_a^T \left(I - J_n \left(J_n^T J_n \right)^{-1} J_n^T \right) Z_x \Delta x. \quad (4)$$

The interpretation of the equation above is that the method projects the target forces f to the null-space of the non-actuated DoFs prior to applying the Jacobian transpose.

In this case, the displayed impedance is:

$$\frac{\partial \tau}{\partial q} = -S^T J_a^T \left(I - J_n \left(J_n^T J_n \right)^{-1} J_n^T \right) Z_x J. \quad (5)$$

In a simple case where Z_x is a uniform stiffness for all DoFs of the virtual object, i.e., $Z_x = k I$, then $\frac{\partial \tau_a}{\partial q_n} = 0$

and all eigenvalues of $\frac{\partial \tau_a}{\partial \mathbf{q}_a}$ are negative, hence passivity is guaranteed. But this is not necessarily the case if the impedance \mathbf{Z}_x is more complex.

In addition, to ensure stability of the rendering, the stiffness of the displayed impedance must be bounded as a function of the sampling rate [5]. As $\frac{\partial \tau}{\partial \mathbf{q}}$ depends on the actuated and non-actuated Jacobians \mathbf{J}_a and \mathbf{J}_n , stability imposes complex nonlinear conditions on the impedance \mathbf{Z}_x . We can conclude that, with null-space force optimization, maximization of rendering transparency depends in a complex nonlinear way on the mapping from device configuration space to virtual configuration space.

Based on these conclusions, instead of just optimizing rendered forces of the standard proxy-based method, we seek a novel rendering method that addresses the challenge of underactuation while remaining passive, and also simplifies maximizing transparency.

V. RENDERING FOR UNDERACTUATED DEVICES

In this section, we propose our novel haptic rendering method for underactuated devices. We first present a nonlinear formulation of a subspace proxy constrained to device DoFs, and we then linearize the problem to yield an efficient rendering method. We conclude with an analysis of the benefits of the method vs. the two methods discussed in the previous section.

A. Subspace Proxy

The rationale of our method is simple. We wish to exploit all benefits of the proxy-based rendering method, namely: (i) accurate visual simulation of the virtual object, (ii) simple rendering of forces based on deviations between proxy and probe, and (iii) simple maximization of transparency by tuning the displayed impedance.

To achieve this, and to circumvent the dimensionality difference of \mathcal{Q} and \mathcal{X} , we define two different proxies. The classical proxy, $\mathbf{x} \in \mathcal{X}$, is a virtual object that is simulated by minimizing the distance to the haptic probe subject to environment constraints; and a *subspace proxy*, $\mathbf{q}^* \in \mathcal{Q}$, is a proxy constrained to the configuration space of the device \mathcal{Q} . Thanks to the classical proxy \mathbf{x} , we retain visual accuracy of the simulation. Thanks to the subspace proxy \mathbf{q}^* , we can compute forces directly based on the deviation $\Delta \mathbf{q}_a = \mathbf{q}_a^* - \mathbf{q}_a$ in the actuated state of the device. And as a corollary, transparency is easily maximized by tuning the display impedance directly on the actuated DoFs.

Given a haptic device state \mathbf{q} , we compute the subspace proxy \mathbf{q}^* by finding the corresponding virtual configuration $f(\mathbf{q}^*)$ that minimizes the distance to the proxy \mathbf{x} . In practice, this is done by solving an optimization problem.

Once the subspace proxy is computed, we can also compute the device force (on the actuated DoFs) τ_a based on a rendering impedance \mathbf{Z}_q and the deviation $\Delta \mathbf{q}_a = \mathbf{S} \Delta \mathbf{q}$ on the actuated DoFs alone. Formally, we define our subspace-proxy-based haptic rendering as follows:

$$\begin{aligned} \tau_a &= \mathbf{Z}_q \mathbf{S} (\mathbf{q}^* - \mathbf{q}), \quad \text{with} \\ \mathbf{q}^* &= \arg \min \| \mathbf{x} - f(\mathbf{q}^*) \|^2. \end{aligned} \quad (6)$$

The main challenge of this formulation is that the mapping f is nonlinear, and finding \mathbf{q}^* requires solving a nonlinear optimization. Next, we relax this challenge.

B. Linearized Subspace Proxy

By linearizing the mapping f at the current device state \mathbf{q} , the optimization problem in (6) turns into a simple quadratic optimization:

$$\begin{aligned} \tau_a &= \mathbf{Z}_q \mathbf{S} \Delta \mathbf{q}, \quad \text{with} \\ \Delta \mathbf{q} &= \arg \min \| \Delta \mathbf{x} - \mathbf{J} \Delta \mathbf{q} \|^2, \end{aligned} \quad (7)$$

with the following closed-form solution:

$$\tau_a = \mathbf{Z}_q \mathbf{S} (\mathbf{J}^T \mathbf{J})^{-1} \mathbf{J}^T \Delta \mathbf{x}. \quad (8)$$

The interpretation of the equation above is that the method projects the proxy deviation $\Delta \mathbf{x}$ onto the device DoFs to compute a subspace proxy deviation prior to the force computation. This implies an important conceptual difference w.r.t. the standard proxy-based rendering method. The standard method transforms forces from the virtual environment to the device, whereas our method transforms displacements and keeps force computation at the device level.

The computational cost of the method is negligible. It requires the solution of a linear system whose size is given by the number of DoFs of the device.

C. Analysis

Similar to Section IV, we analyze the displayed impedance, which in this case is:

$$\frac{\partial \tau}{\partial \mathbf{q}} = -\mathbf{S}^T \mathbf{Z}_q \mathbf{S}. \quad (9)$$

This impedance yields two notable results. First, passivity is easily enforced, simply by ensuring that the rendering impedance \mathbf{Z}_q is positive definite. Second, transparency is easily maximized, simply by setting the stiffness terms in \mathbf{Z}_q to the maximum allowed by stability constraints. Unlike the methods studied in Section IV, the displayed impedance is not affected by configuration-dependent scaling factors.

VI. RESULTS

A. Device

As a benchmark for our rendering method, we have used a single finger component of an underactuated hand exoskeleton. The device applies only normal forces to the finger phalanges during flexion/extension of the fingers, and these forces are distributed by a single linear actuator. Fig. 3-right shows the kinematics of the device, where the linear actuator (Firgelli L16) with displacement $\mathbf{q}_a = (l_x)$ provides rotation to the MCP and PIP joints $\mathbf{x} = (q_{01}, q_{02})^T$. The underactuation property distributes the actuator's force based on contact forces, allowing for automatic adjustment for different tasks (see [27] for further information). The mechanism includes a potentiometer (see Fig. 3-left) to measure a non-actuated joint $\mathbf{q}_n = (q_B)$ and achieve pose estimation of the finger joints throughout the operation [26].

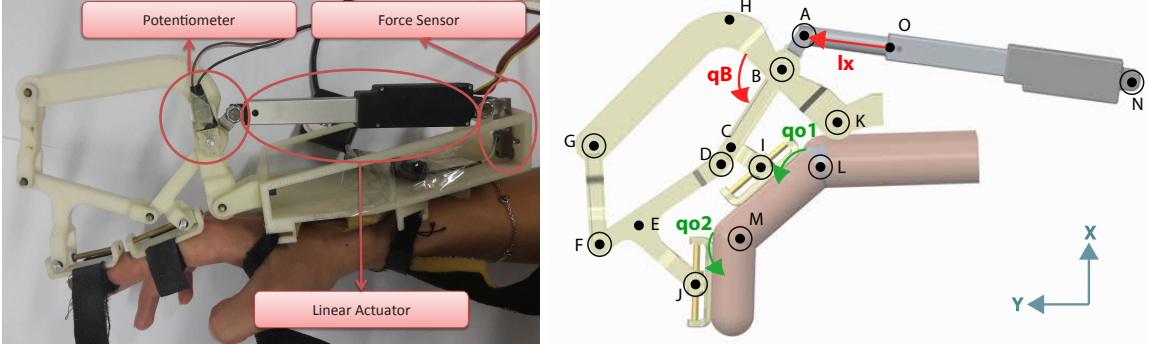


Fig. 3. Left: The underactuated exoskeleton used as benchmark, indicating its linear actuator and various sensors. Right: Schematic representation of the kinematic structure, including the device DoFs (l_x actuated and q_B non-actuated) and the end-effector DoFs (q_{o1} MCP joint and q_{o2} PIP joint).

A Delfino board has been used to control the device and read the sensors through ADC pins with 1 kHz frequency. The communication between the host computer and the control board is set by a simple USB port, which limits the communication speed to 500 Hz . The desired actuator force τ_a , which is calculated by the optimization process, is used directly as the reference input for a closed-loop force control algorithm, while the actual forces are measured thanks to the force sensor shown in Fig. 3-left.

B. Virtual Environment

We render virtual interactions between a soft finger model [21] and other objects, as shown in Fig. 1 and the accompanying video. We track the motion of the palm with a LeapMotion device, and we integrate it with the tracking of the finger provided by the exoskeleton. This combined tracking sets the configuration \mathbf{q} of the device, which we transform into the probe representation of the phalanges $f(\mathbf{q})$ using the two joints mentioned above. We model contact between the soft finger and other objects, thus constraining the proxy phalanges, and then apply our rendering algorithm to compute the device force command.

C. Experiments

We have recorded several finger trajectories and their associated rendering computations. For the experiments, we have used as impedance a normalized stiffness to factor out the average scale in \mathbf{J}_a , i.e., $Z_q = 1$ and $Z_x = \frac{1}{\text{avg}(\|\mathbf{J}_a\|)^2} \mathbf{I}$. To compare our subspace rendering method with the standard and null-space methods, we carry out force computation and impedance analysis in a controlled setting. Given a recorded finger trajectory, we fix the proxy at $\mathbf{x} = 0$, and we compute the output force on the linear actuator, as well as the displayed impedance $\frac{\partial \tau_a}{\partial \mathbf{q}_a}$. We compute this impedance (a) following the theoretical formulations in (2), (5), and (9) respectively for the three rendering methods, and (b) through finite differences of the applied force and the device motion between frames, i.e., $\frac{\Delta \tau_a}{\Delta \mathbf{q}_a}$.

Fig. 4 shows the results for a sample finger trajectory. Our subspace-proxy-based method is always passive in the experiment, according to the theoretical result but also in practice. The standard and null-space methods, on the other

hand, are not always passive in practice. This contradicts the theoretical results, due to the missing $\frac{\partial \mathbf{J}}{\partial \mathbf{q}}$ term.

VII. CONCLUSIONS AND FUTURE WORK

In this paper we have analyzed the problem of haptic rendering on underactuated devices, considering generic kinematic relationships between the haptic device and the virtual world. To address this problem, we propose a novel haptic rendering method, which extends the classic proxy-based method with a subspace proxy to enable an efficient mapping between configuration spaces. Our theoretical analysis indicates that the proposed method offers superior passivity and transparency properties. We have also validated the results on an underactuated hand exoskeleton.

Our novel rendering method opens up multiple avenues for further investigation. First, our rendering algorithm linearizes the mapping from device to virtual workspace, which works well when the deviation between device state and subspace proxy is small. A full nonlinear solve would be more robust under large proxy deviations, but it requires efficient solution methods. Second, in our impedance analysis we have made two important approximations, namely that the proxy remains still and that the Jacobian of the mapping from device to virtual workspace is constant. A passivity controller could be needed to enforce passivity in all cases. And third and most important, the overall quality of haptic rendering can be optimized in a task- and device-specific manner by tuning the objective functions that guide the computation of the proxy and the subspace proxy.

ACKNOWLEDGEMENTS

We would like to thank the anonymous reviewers for their helpful comments. This project was supported in part by grants from the EU (FP7 project no. 601165 WEARHAP, H2020 project no. 644839 CENTAURO), and the Spanish Ministry of Economy (TIN2015-70799-R).

REFERENCES

- [1] R. J. Adams and B. Hannaford. Stable haptic interaction with virtual environments. *IEEE Transactions on Robotics and Automation*, 15(3):465–474, 1999.

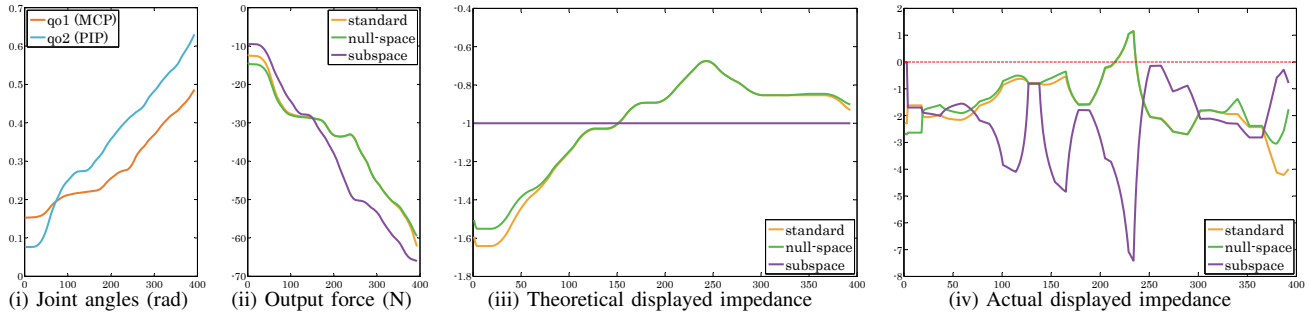


Fig. 4. Performance comparison of the three rendering methods discussed in the paper (standard, null-space, and subspace). In the test, the proxy is kept still at a zero angle, and the rendering impedances are normalized to factor out the average scale in \mathbf{J}_a . From left to right: (i) Motion of the joint angles; (ii) Output force for the three methods; (iii) Theoretical displayed impedance; and (iv) impedance displayed in practice. With our subspace method, the displayed impedance is always negative, and hence the rendering is passive.

- [2] F. Barbagli and K. Salisbury. The effect of sensor/actuator asymmetries in haptic interfaces. In *11th Symposium on Haptic Interfaces for Virtual Environment and Teleoperator Systems, 2003. HAPTICS 2003. Proceedings.*, pages 140–147, 2003.
- [3] J. Barbić and D. James. Time-critical distributed contact for 6-Dof haptic rendering of adaptively sampled reduced deformable models. In *2007 ACM SIGGRAPH / Eurographics Symposium on Computer Animation*, pages 171–180, Aug. 2007.
- [4] L. Birglen, T. Laliberté, and C. Gosselin. Design and control of the laval underactuated hands. In *Underactuated Robotic Hands*, pages 171–207. Springer Berlin Heidelberg, 2008.
- [5] J. E. Colgate and J. M. Brown. Factors affecting the z-width of a haptic display. In *Proceedings of the 1994 IEEE International Conference on Robotics and Automation*, pages 3205–3210 vol.4, 1994.
- [6] J. E. Colgate, M. C. Stanley, and J. M. Brown. Issues in the haptic display of tool use. *Proc. of IEEE/RSJ International Conference on Intelligent Robots and Systems*, pages pp. 140–145, 1995.
- [7] H. G. Differ. Design and Implementation of an Impedance Controller for Prosthetic Grasping. Master’s thesis, University of Twente, the Netherlands, 2010.
- [8] C. Duriez, F. Dubois, A. Kheddar, and C. Andriot. Realistic haptic rendering of interacting deformable objects in virtual environments. *Proc. of IEEE TVCG*, 12(1), 2006.
- [9] A. Fassih, D. S. Naidu, S. Chiu, and P. Kumar. Design and control of an underactuated prosthetic hand. In *Proceedings of the 11th International Conference on Applications of Electrical and Computer Engineering, ACA’12*, pages 77–82, 2012.
- [10] C. Garre, F. Hernandez, A. Gracia, and M. A. Otraduy. Interactive simulation of a deformable hand for haptic rendering. In *Proc. of World Haptics Conference*, 2011.
- [11] S. S. Hasan, S. M. Nacy, E. E. Eldukhri, H. G. Kamil, and E. H. Flaieh. Position control of linkage underactuated robotic hand. *Control Theory and Informatics*, 5(3), 2015.
- [12] P. Kadlecák, P. Kmoch, and J. Krivánek. Haptic rendering for under-actuated 6/3-dof haptic devices. In *Haptics: Neuroscience, Devices, Modeling, and Applications: 9th International Conference, EuroHaptics 2014, Versailles, France, June 24–26, 2014, Proceedings, Part II*, pages 63–71. Springer Berlin Heidelberg, 2014.
- [13] T. Laliberte, L. Birglen, and C. Gosselin. Underactuation in robotic grasping hands. *Machine Intelligence & Robotic Control*, 4(3):1–11, 2002.
- [14] L. Lee. Rendering 6-DOF Object-to-Object Interaction with 3-DOF Haptic Interfaces. Master’s thesis, TU Delft, the Netherlands, 2014.
- [15] G. R. Luecke. Haptic interactions using virtual manipulator coupling with applications to underactuated systems. *IEEE Transactions on Robotics*, 27(4):730–740, 2011.
- [16] H. Luo, X. Duan, and H. Deng. Sliding mode impedance control of a underactuated prosthetic hand. In *2014 IEEE International Conference on Information and Automation (ICIA)*, pages 726–729, 2014.
- [17] W. A. McNeely, K. D. Puterbaugh, and J. J. Troy. Six degrees-of-freedom haptic rendering using voxel sampling. In *Proc. of SIGGRAPH 99, Computer Graphics Proc.*, pages 401–408, Aug. 1999.
- [18] L. Meli and D. Prattichizzo. *Task-Oriented Approach to Simulate a Grasping Action Through Underactuated Haptic Devices*, pages 249–257. Springer Berlin Heidelberg, Berlin, Heidelberg, 2014.
- [19] M. Ortega, S. Redon, and S. Coquillart. A six degree-of-freedom god-object method for haptic display of rigid bodies with surface properties. *IEEE Transactions on Visualization and Computer Graphics*, 13(3):458–469, 2007.
- [20] M. Otraduy, C. Garre, and M. Lin. Representations and algorithms for force-feedback display. *Proceedings of the IEEE*, 101(9):2068–2080, Sept 2013.
- [21] A. G. Perez, G. Cirio, F. Hernandez, C. Garre, and M. A. Otraduy. Strain limiting for soft finger contact simulation. In *World Haptics Conference (WHC), 2013*, pages 79–84, 2013.
- [22] A. G. Perez, G. Cirio, D. Lobo, F. Chinello, D. Prattichizzo, and M. A. Otraduy. Efficient nonlinear skin simulation for multi-finger tactile rendering. In *2016 IEEE Haptics Symposium (HAPTICS)*, pages 155–160, 2016.
- [23] A. G. Perez, D. Lobo, F. Chinello, G. Cirio, M. Malvezzi, J. S. Martín, D. Prattichizzo, and M. A. Otraduy. Soft finger tactile rendering for wearable haptics. In *2015 IEEE World Haptics Conference (WHC)*, pages 327–332, 2015.
- [24] P. Rea. On the design of underactuated finger mechanisms for robotic hands. In *Advances in Mechatronics*. InTech, 2011.
- [25] D. C. Rusipini, K. Kolarov, and O. Khatib. The haptic display of complex graphical environments. In *Proceedings of the 24th Annual Conference on Computer Graphics and Interactive Techniques, SIGGRAPH ’97*, pages 345–352, 1997.
- [26] M. Sarac, M. Solazzi, D. Leonardi, E. Sotgiu, M. Bergamasco, and A. Frisoli. Design of an underactuated hand exoskeleton with joint estimation. In G. Boschetti and A. Gasparetto, editors, *Advances in Italian Mechanism Science: Proceedings of the First International Conference of IFToMM Italy*, pages 97–105. Springer International Publishing, 2017.
- [27] M. Sarac, M. Solazzi, E. Sotgiu, M. Bergamasco, and A. Frisoli. Design and kinematic optimization of a novel underactuated robotic hand exoskeleton. *Meccanica*, pages 1–13, 2016.
- [28] L. N. Verner and A. M. Okamura. Sensor/actuator asymmetries in telemanipulators: Implications of partial force feedback. In *2006 14th Symposium on Haptic Interfaces for Virtual Environment and Teleoperator Systems*, pages 309–314, 2006.
- [29] L. N. Verner and A. M. Okamura. Force & torque feedback vs force only feedback. In *World Haptics 2009 - Third Joint EuroHaptics conference and Symposium on Haptic Interfaces for Virtual Environment and Teleoperator Systems*, pages 406–410, 2009.
- [30] D. Wang, Y. Shi, S. Liu, Y. Zhang, and J. Xiao. Haptic simulation of organ deformation and hybrid contacts in dental operations. *IEEE Transactions on Haptics*, 7(1):48–60, 2014.
- [31] D. Wang, X. Zhang, Y. Zhang, and J. Xiao. Configuration-based optimization for six degree-of-freedom haptic rendering for fine manipulation. *Haptics, IEEE Transactions on*, 6(2):167–180, 2013.
- [32] H. Xu and J. Barbić. Adaptive 6-dof haptic contact stiffness using the gauss map. *IEEE Transactions on Haptics*, 9(3):323–332, 2016.
- [33] C. Zilles and J. Salisbury. A constraint-based god-object method for haptic display. In *Intelligent Robots and Systems 95. ‘Human Robot Interaction and Cooperative Robots’, Proceedings. 1995 IEEE/RSJ International Conference on*, volume 3, pages 146–151 vol.3, 1995.